BAV MAGAZINE SPECTROSCOPY

VV Cephei - Campaign after Eclipse 2018

Ernst Pollmann (ernst-pollmann@t-online.de)

Abstract

None of the studies or work published so far has been able to clearly demonstrate which of the individual components of the binary system VV Cephei, such as the B companion, the accretion disk or the emission lobes, produces the residual Hα emission during the phase of total solar eclipse. The model recently proposed by Pollmann & Bennett suggested that only the upper emission lobe (blue emission V of the Hα components), which is bound with the rotation axis of the B companion star and its accretion disk can be solely responsible for this residual emission. *Part I*: With continued observations 4 years after the end of the eclipse in December 2018, we found that from the partial eclipse of the emission lobes and the total eclipse of the B star plus disk through the M star, the Hα EW with the period of 43 days and the significantly smallest amplitude (compared to the EW of the following later sections) explaines the residual emission. *Part II* documents the duration of the partial eclipse of the Hα emission flux (components V+R) as well as the total UV flux eclipse through the M star and the analysis of the quasi-periodic variations of their time behavior. *Part III* describes the period analysis of the V/R variations from November 2000 to February 2023. The sinusoidal amplitude of the linear detrended V/R data of the two emission lobes V and R in Fig. 10 clearly demonstrates the Kepler orbital period of 7430 days with an average amplitude of (+/-) 0.33.

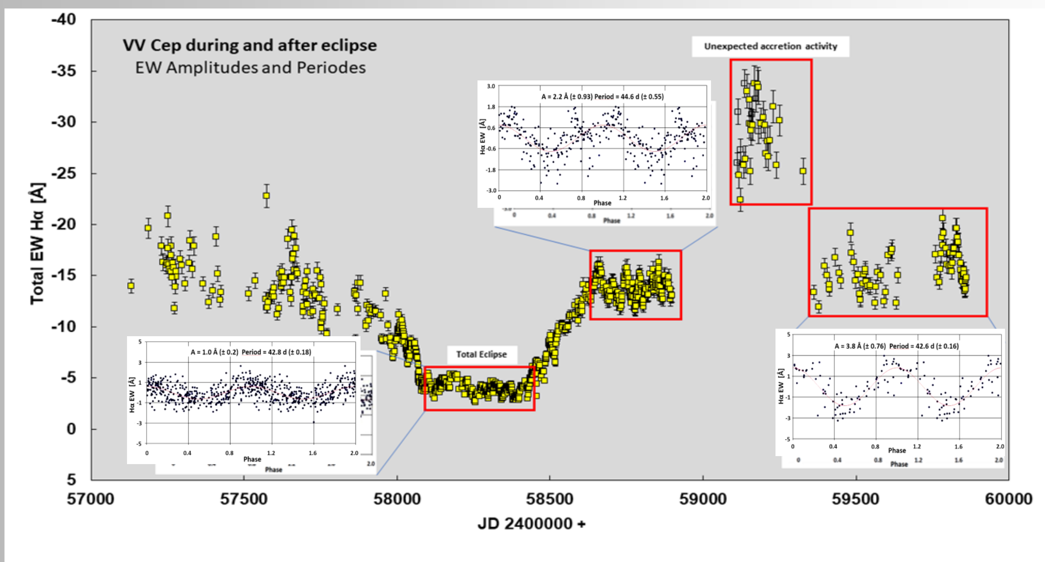

Fig. 1: Overview of the campaign to detect the rotation axis precession of the B star with Hα-EW periodicity as indicator of three observation sections

In this project it was particularly important to use a uniform evaluation program to determine the Hα-EW in the spectra of different observers, which were obtained with different spectrographs, i.e. with different spectral resolutions between 10000 and 20000. This heterogeneity required a high level of accuracy in uniform wavelength scaling, normalization of the continuum, and fixed definition of the EW integration region. These requirements are given by using the program SPECTRO-CALC (https://www.astrophoto.at). Figure 2 describes the EW integration range as well as the spectral lines that were used for the uniform post-calibration of all spectra.

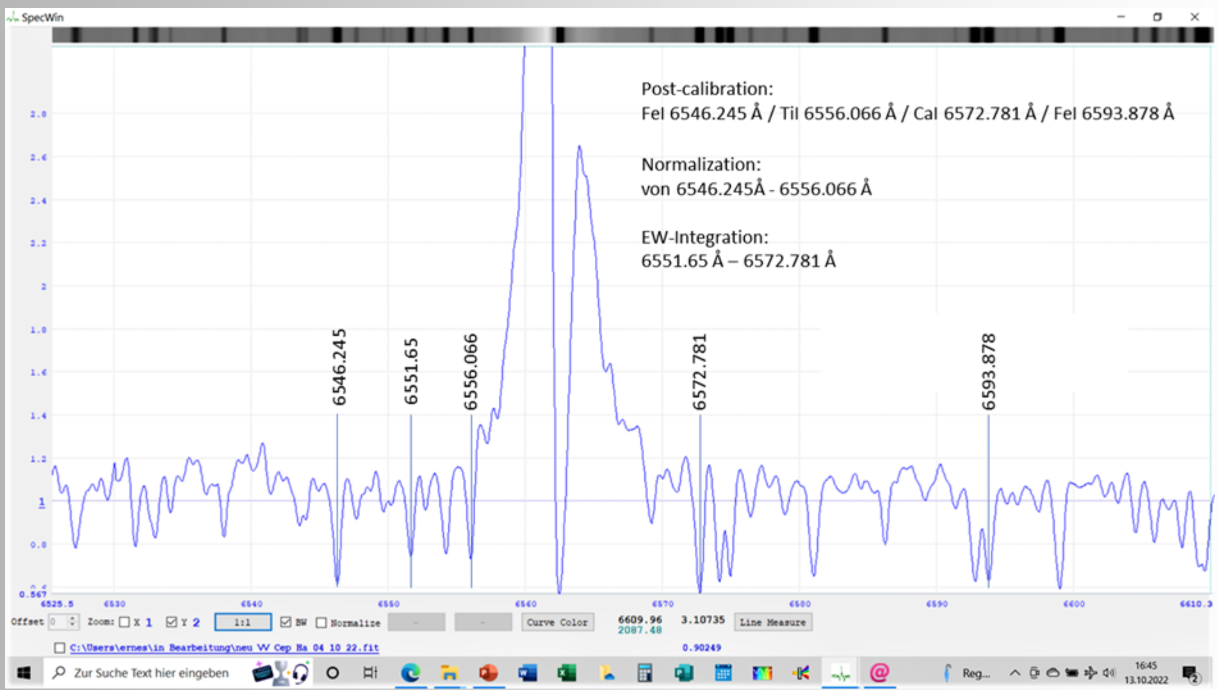

Fig. 2: Description of selected wavelengths for recalibration, continuum normalization and the EW integration range.

The wavelength calibration was carried out at the wavelengths FeI 6546.245Å / TiI 6556.066Å / CaI 6572.781Å / FeI 6593.878Å recommended by Hutchings & Wright (1971) as suitable in the spectrum of the M supergiant. The normalization was performed in the range of 6546.245Å - 6556.066Å.

The EW integration area extended from 6551.65Å – 6572.781Å. The measurement accuracy of the wavelength calibration was consistently in the range of (±) 0.005Å. The accuracy of the determination of the EW can be given as (±) 0.3Å in terms of reproducibility measurements. In this respect, precise prerequisites were given with which the project could be carried out.

Results

In the following, the analyzes of the periodicity and amplitudes of the Hα-EW will be presented. First, Figure 3 describes the phase diagram of the period analysis of the total eclipse section of JD 2458068-58441. With a period of 42.8 d (± 0.18), the Hα-EW varies with an amplitude of 1.0 Å (± 0.2).

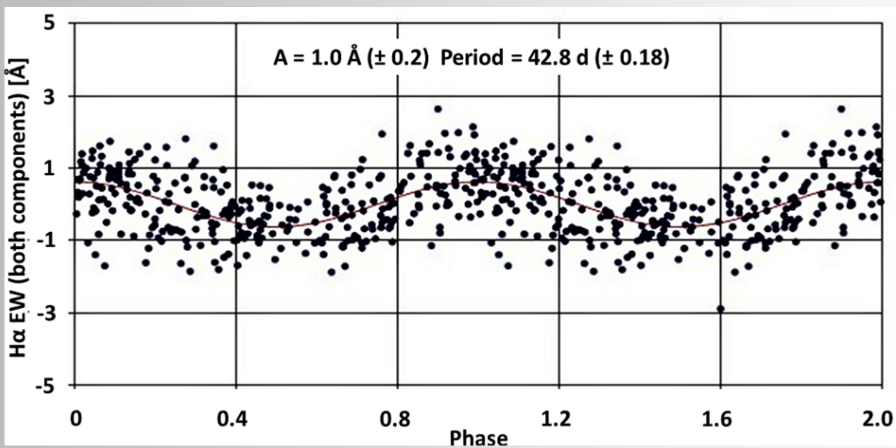

Fig.3: Evaluation of the Hα-EW period and the amplitude for the section of total eclipse of JD 2458068-58441 (see also Fig. 1)

Figure 4 describes the phase diagram of the periodicity and amplitude of the Hα-EW for the section JD 2458663-58897 outside the total eclipse. With a period of 44.6 d (± 0.55), the Hα-EW varies with an amplitude of 2.2 Å (± 0.93).

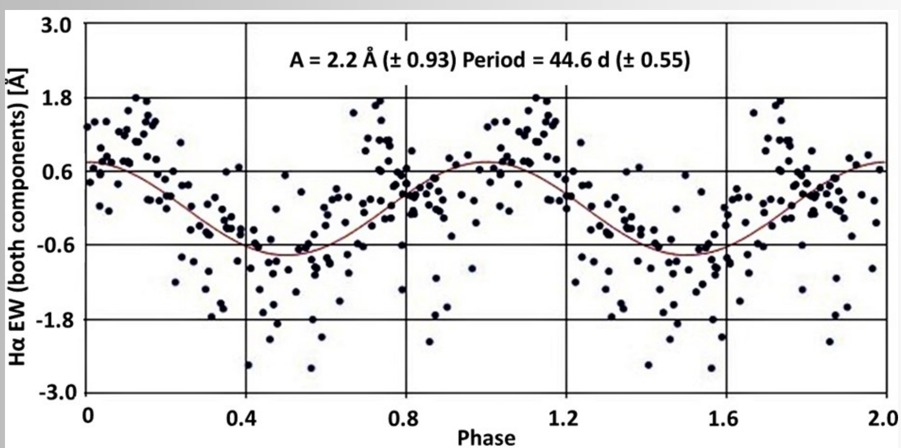

Fig. 4: Evaluation of the Hα-EW period and the amplitude for the section outside the total eclipse of JD 2458663-58897 (see also Fig. 1)

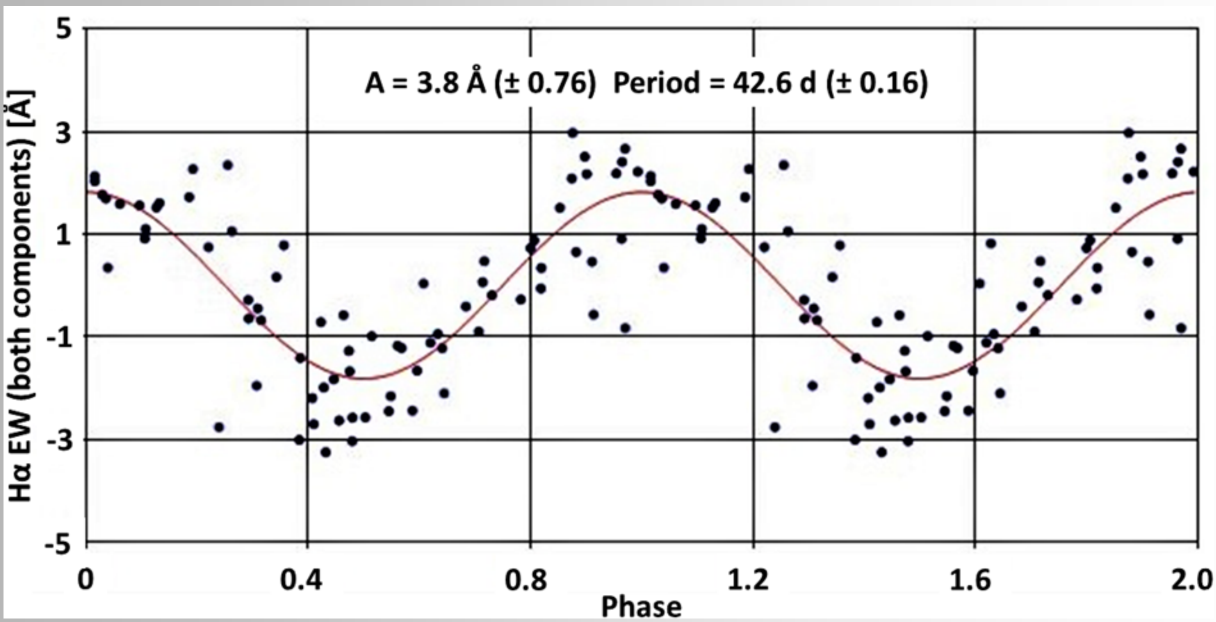

Fig. 5: Evaluation of the Hα-EW period and the amplitude for the section outside the eclipse of JD 242459363-59637 (see also Fig. 1)

The data of these three periods analyzes are summarized in the table below:

Time section	Hα-EW Amplitude [Å]	Period [d]
JD 2458068-58441	1.0 (± 0.2)	42.8 (± 0.18)
JD 2458663-58897	2.2 (± 0.93)	44.6 (± 0.55)
JD 2459363-59637	3.8 (± 0.76)	42.6 (± 0.16)

For the investigation period JD 2458068 to JD 2459637 (= 4.3 years) an average period of Hα EW of 43.3 days (± 0.3) was found. This is also their typical period because of the coupling of the two emission lobes with the rotational axis of the B star.

Fig. 6 shows the Hα line flux of both emission components V+R along with UV flux represented by Umag measurements. In the U-band, most of the flux is believed to come from the hot components of the binary system - the B star and its precessing accretion disk. Umag brightness measurements during the phase of the *total eclipse* documents almost the complete disappearance of UV flux of the B star plus its accretion disk by the M star.

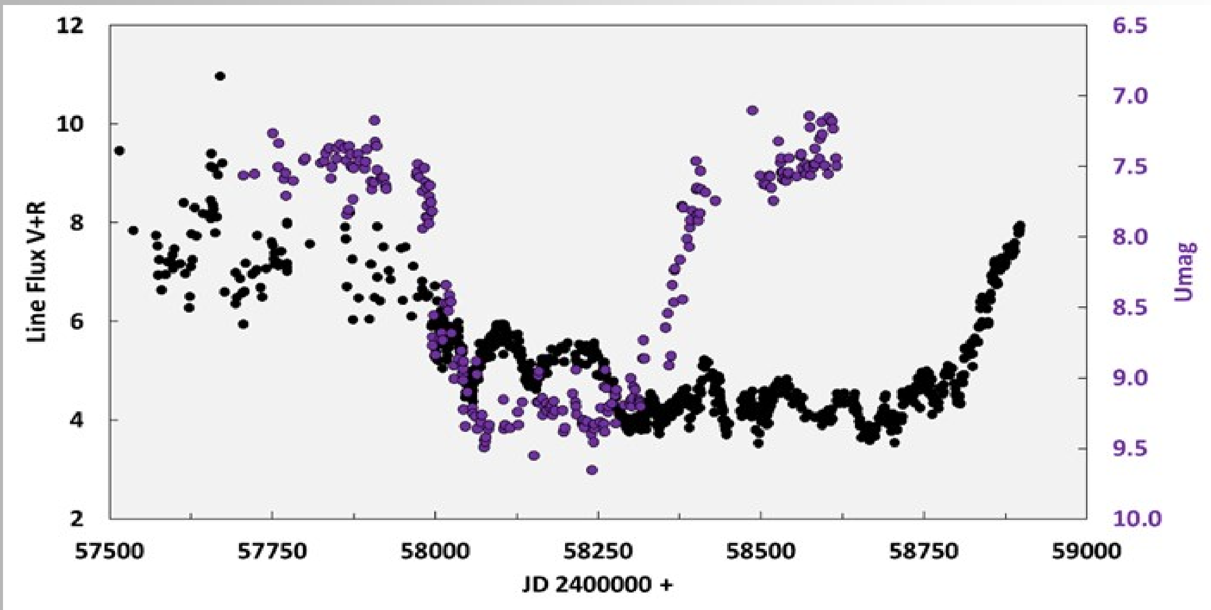

Fig. 6: *Total eclipse* of the B star plus disk (JD 2457972-58486) represented by Umag (https://bav-astro.eu/index.php/veraenderliche/bedeckungsveraenderliche/vv-cep-kampagne) and *the partial eclipse* of the Hα line flux of the emission components V+R (JD 2457500-58895)

But in the observer's line of sight, the emission sources V+R, and their coupling to the rotation axis of the B star, extend far beyond the diameter of the supergiant, resulting only in a partial eclipse by the M star. Contrary to our earlier assumption, we can say now, that the partial eclipse of the components V and R by the M star is responsible for the residual emission during the total eclipse.

Both fluxes, Hα (V+R) as well the UV (B star plus disk), are subject an additional orbital precession of the rotation axis of the B star. This is easy to recognize as quasi-periodic variation of its time behavior in Fig. 6. A period analysis of its detrended data is shown in Fig. 7a-d.

The Umag analysis of the polynomially detrended data (degree 15) in figure 7b results in a period of 162.5 d (±3.5). The analysis of the detrended V+R data in figure 7d results in a period of 151.2 d (±1.0). The average period from both thus leads to 157 d. The difference of about 10 days between these two periods is most likely due to the relatively small amount of Umag data.

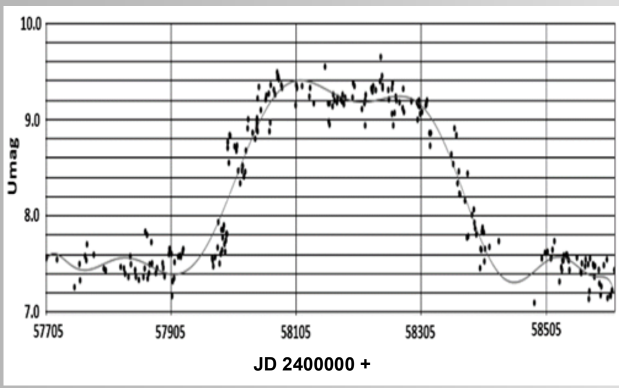

Fig. 7a: Umag measurements during total eclipse

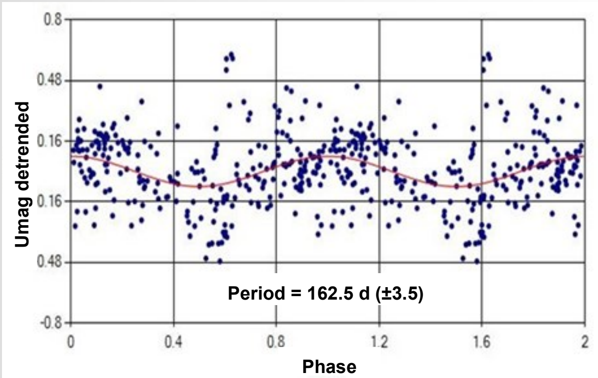

Fig. 7b: Umag period analysis of the polynominal (degree 15) detrended data of Fig. 7a
P = 162.5 d (±3.5)

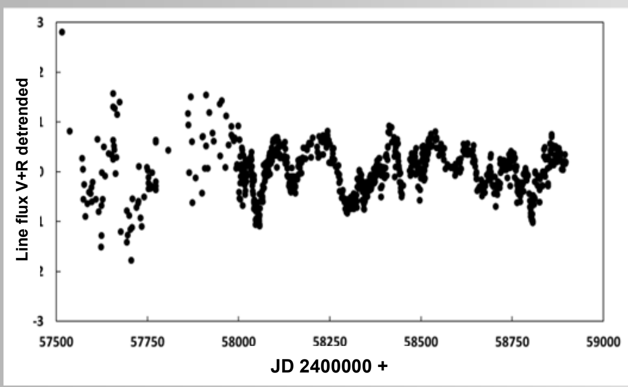

Fig. 7c: Hα line flux V+R polynominal (degree 3) detrended

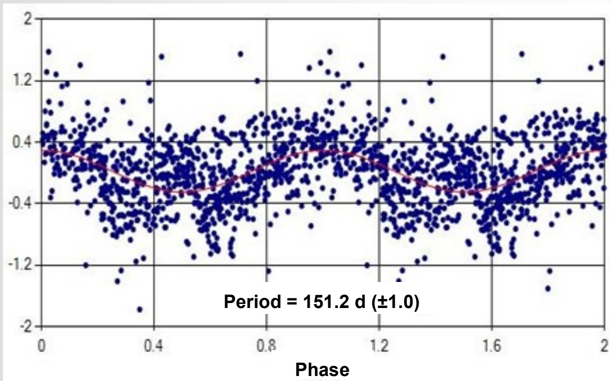

Fig. 7d: Period analysis of the detrended data in Fig. 7c; P = 151.2 d (±1.0)

Note that the 43d EW period is about ¼ of the 162.5 d period. It is not clear yet how this is to be interpreted. Observations during the following orbital sections of the B star may lead to an explanation.

Part III

The 43.3 d EW period of the blue (V) and red (R) emission lobes described in Part I and their coupling with the precessing rotation axis of the B star naturally led to the question of their behavior in the orbital phases periastron and apastron. Figure 8 shows the monitoring of the V/R ratio of the first campaign from November 2000 to February 2023. The blue stripes mark the orbital phases periastron and apastron with a period of 7430 days (Wright, 1977).

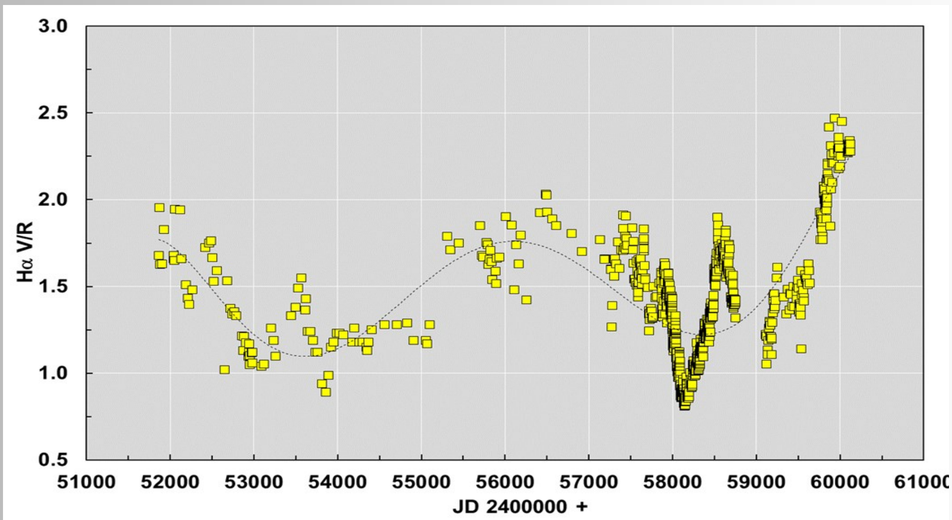

Fig. 8: Time behavior of the ratio V/R of the first campaign November 2000 to February 2023

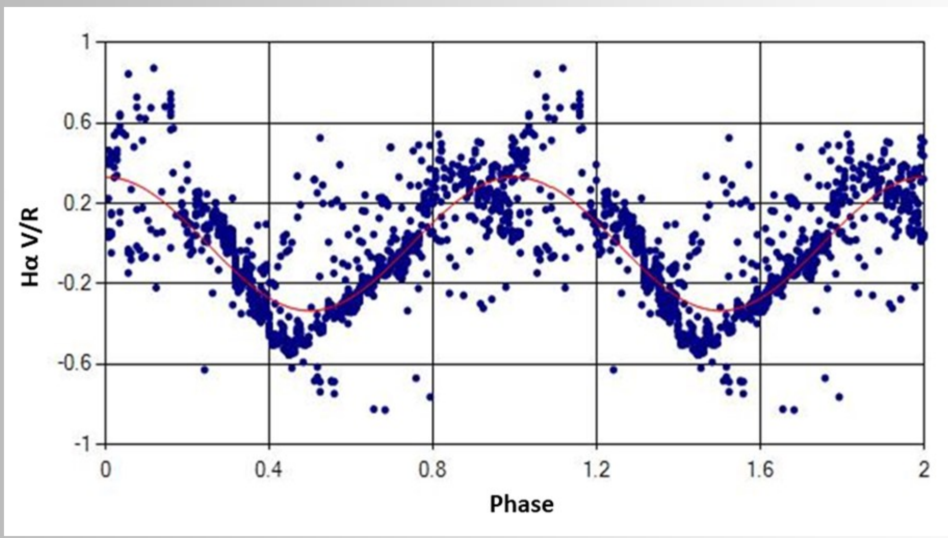

Fig. 9: Phase diagram of the campaign November 2000 to February 2023; Period = 7443d (Wright 1977; P = 7450d; T = 2438389 (± 60)

To demonstrate the ratio V/R in the B star's Kepler-orbital context, a period analysis was performed of the polynominal detrended data in Figure 8. In the sinusoidal phase diagram of this analysis in Fig. 9 (red curve), the periastron has to be assigned at phase 1.0, the apastron at phase 0.5.

Conclusion

With the present, renewed investigation campaign, the precession period of 43.8 d (± 0.1) derived from the radial velocity of the blue emission component published by Pollmann (2022) is very well confirmed with the averaged Hα-EW period of 43.3 d (± 0.3) during the total eclipse as well as out of the eclipse.

The tabular comparison of the Hα-EW amplitudes also shows that, contrary to the assumptions of Pollmann & Bennett (2020), the observed residual emission during the period of the total eclipse (JD 2458068-58441) have been generated from both emission lobes (V+R) in the disk rotation axis of the B star.

The coupling of the emission sources V+R with the rotational axis of the B star extends far beyond the diameter of the supergiant in the observer’s line of sight. This results in only a partial eclipse through the M supergiant, and hence to the residual emission during the total eclipse. This claim is strongly supported by photomultiplier brightness measurements in U, which support the complete disappearance of the B star during the total eclipsing phase.

Continued monitoring the B star’s approaching periastron phase in 2025 will determine the effect of the precession of the B Star’s rotation axis and whether it can be observed in this form in further orbital phases The sinusoidal amplitude of the linear detrended V/R data of the two emission lobes V and R in Fig. 9 clearly demonstrates the Kepler orbital period of 7430 days with an average amplitude of (+/-) 0.33.

The precessing rotation axis of the B star with the coupled emission components V and R is characterized by two superimposed periods: the short-term precession period with P = 43 days and an (averaged) precession period with P = 157 days. The present results imply that both periods remain during a complete orbit of the B star. Although the 43-day period of the B star's rotation axis is triggered by the M supergiant, the excitation process for the 157-day period remains unclear.

Acknowledgement

I am very grateful to all observers of the ARAS spectroscopy group for their provided spectra of Figs. 1 and 8, and particularly A. Stiewing for his kindly improvement of this paper.

References

Hutchings, J. B., and Wright, K. O., 1971, Mon. Not. Roy. Astron. Soc., 155, 203.
Pollmann, E., and Bennett, P. D. 2020, J. Amer. Assoc. Var. Stars, 48
Pollmann, E., 2022, J. Amer. Assoc. Var. Stars, 50
SPECTRO-CALC (https://www.astrophoto.at)
Wright, K. O., 1977JRASC..71..152W (harvard.edu)